Localized states in a triangular set of linearly coupled complex Ginzburg-Landau equations

Ariel Sigler and Boris A. Malomed
Department of Interdisciplinary Studies, School of Electrical Engineering, Faculty of Engineering, Tel Aviv University, Tel Aviv 69978, Israel

Dmitry V. Skryabin
Centre for Photonics and Photonic Materials, Department of Physics, University of Bath, Bath BA2 7AY, United Kingdom
(Received 2 September 2006; published 12 December 2006)

We introduce a pattern-formation model based on a symmetric system of three linearly coupled cubic-quintic complex Ginzburg-Landau equations, which form a triangular configuration. This is the simplest model of a multicore fiber laser. We identify stability regions for various types of localized patterns possible in this setting, which include stationary and breathing triangular vortices.

DOI: 10.1103/PhysRevE.74.066604 PACS number(s): 05.45.Yv, 42.81.Dp, 42.55.Wd, 42.55.Tv

I. INTRODUCTION AND THE MODEL

Universal models describing formation of localized states (LSs) and extended patterns in dissipative nonlinear media are based on complex Ginzburg-Landau (CGL) equations. These models are interesting in their own right [1,2], and in terms of applications to nonlinear optics, hydrodynamics, reaction-diffusion systems, etc. [2,3].

Stationary or oscillatory LSs are the most fundamental solutions to CGL equations. In the application to nonlinear optics, they represent pulses generated by fiber lasers [4]. Exact solutions for pulses are available in the CGL equation with the simplest cubic nonlinearity [5], but they are unstable (more sophisticated LSs were found in two-dimensional models of laser cavities [6]). A straightforward modification of the equation, aimed at creation of stable LSs, is provided by the cubic-quintic (CQ) nonlinearity, with linear loss and cubic gain (rather than the linear gain and cubic loss, as in the ordinary cubic CGL equation), and additional quintic loss that provides for the overall stability. The CQ CGL equation was first introduced in Ref. [7], and its stable LS solutions were predicted, using an analytical approximation, in Ref. [8]. Later, LSs and their stability in this model were investigated in detail [9,10].

Stable pulses may also be found in a model with the cubic nonlinearity (without higher-order terms), composed of the cubic CGL equation linearly coupled to an extra linear equation with the loss term [11]. This system gives rise to exact analytical solutions for stable LSs [12], and (numerically found) breathers, i.e., randomly oscillating (and walking, in the general case) robust pulses [13].

Linearly coupled CGL equations supply a model for ring lasers based on dual-core optical fibers [11,14], and are noteworthy dynamical systems by themselves [15]. However, the above-mentioned stable LSs were previously found only in strongly asymmetric dual-core models, with gain in one core, and loss in the other (otherwise, LSs cannot be stable) [11–13]. It is natural to look for symmetric and asymmetric stable LSs in *symmetric* dual-core (*twin-core*, in that case) models. This was done in recent work [16], where four species of stable LSs had been identified, by dint of systematic numerical analysis: breathers and three kinds of stationary LSs, *viz.*, symmetric and asymmetric ones, and *split pulses*, the states of the latter type featuring a separation between centers of the two components.

Recently, new designs of fiber lasers with dozens of cores have been worked out [17]. In particular, a distinctive feature of necklace-shaped fiber sets, consisting of $N \geqslant 3$ cores placed along a circumference, is a possibility of the existence of *vortex modes* in them, which we realize as states with the phase difference of $2\pi/N$ between adjacent cores, the respective phase change along the full circle being $\Delta\phi = 2\pi$. If $\Delta\phi$ is a multiple of 2π, it corresponds to a higher-order vortex. These structures resemble vortex-carrying circularly arranged clusters of localized states in a two-dimensional CGL model [18], since a chain of linearly coupled CGL equations may be considered as a discrete version of a single continuous higher-dimensional equation.

In this paper, our aim is to report a comprehensive chart of various stable LS states, including vortices, that exist in the triangular set of CQ CGL equations, which is the simplest version of the above-mentioned necklace arrangement. Accordingly, the model is a system of three CQ CGL equations, each one being symmetrically coupled by linear terms to its two neighbors,

$$iU_z + \tfrac{1}{2}U_{tt} + |U|^2U = i\delta U + i\epsilon|U|^2U + i\beta U_{tt} - (i\mu - \nu)|U|^4U - \kappa(V + W), \tag{1}$$

$$iV_z + \tfrac{1}{2}V_{tt} + |V|^2V = i\delta V + i\epsilon|V|^2V + i\beta V_{tt} - (i\mu - \nu)|V|^4V - \kappa(W + U), \tag{2}$$

$$iW_z + \tfrac{1}{2}W_{tt} + |W|^2W = i\delta W + i\epsilon|W|^2W + i\beta W_{tt} - (i\mu - \nu) \times |W|^4W - \kappa(U + V). \tag{3}$$

This system models a structured fiber with three cores forming an equilateral triangle. The equations are written in the usual fiber-optics notation, with U, V, and W being complex amplitudes of the electromagnetic waves in three cores, z and t the propagation distance and reduced time, and the coefficient in front of the Kerr terms (nonlinear terms on the left-hand side of the equations) scaled to be 1. Anomalous group-velocity dispersion, which facilitates the creation of solitons, is assumed by setting the coefficients in front of the second

derivatives on the left-hand side to be +1/2. Real constants $-\delta$, μ, and ϵ account for the linear and quintic loss and cubic gain, respectively (therefore, we assume $\delta \leqslant 0$ and $\mu, \epsilon > 0$), and $\beta > 0$ is a spectral-filtering coefficient, which accounts for the dispersive linear loss. The quintic correction to the Kerr nonlinearity, with coefficient ν, is also included. We assume $\nu \geqslant 0$, as such corrections to the nonlinear response of self-focusing optical media were experimentally found to be self-defocusing [19]. Finally, real κ accounts for the linear cyclic coupling between the three cores. We use the residual scaling invariance of Eqs. (1)–(3) to fix $\mu \equiv 0.1$.

Note that solitons in conservative models of triangular configurations formed by ordinary nonlinear fibers, and by fiber Bragg gratings (FBGs), have been previously studied in Refs. [20,21], respectively. Various types of symmetric and asymmetric soliton states in the triangular systems were found in these works (in Ref. [21], the stability of the respective solutions was investigated too); however, triangular vortex-soliton complexes were not considered previously.

The rest of the paper is organized as follows. In Sec. II, we present a generic example of a diagram in the plane of (δ, κ), that shows different species of stable LSs that are possible in the present system. The diagram readily features bistability and tristability. In Sec. III, nonvortical states (symmetric and asymmetric ones, including breathers) are considered in detail. Section IV provides for a detailed description of vortices (including vortical breathers). The paper is concluded by Sec. V.

II. THE PARAMETER CHART OF LOCALIZED-STATE COMPLEXES

Searching for stable LSs in coupled CGL equations is facilitated by the fact that they are *attractors*, hence they can be found from direct simulations of Eqs. (1)–(3) (we are interested in attractors which represent localized solutions, but they are not necessarily stationary—as shown below, they may feature periodic or chaotic intrinsic dynamics). In the case of multistability, the attractor revealed by the simulations depends on the initial configuration. Here, we present a chart of LS states in the plane of (δ, κ), i.e., the linear-loss and linear-coupling constants. In particular, in the fiber-laser setup δ may be easily varied by adjusting the pump. The chart is displayed in Fig. 1 for $\nu = 0.1$ and $\epsilon = \beta = 0.5$ in Eqs. (1)–(3) (recall $\mu \equiv 0.1$ was fixed by scaling). Simulations performed at other values of the parameters demonstrate that this example is quite a generic one (the results might be essentially different for $\beta = 0$, when, due to the absence of the dispersive loss, LSs are mobile [10]; however, stable LSs could not be found in the present model with $\beta = 0$).

To include all possible types of stable LSs at given values of the parameters, the simulations were run, until an established state could be identified, starting from initial configurations of several different types. These were composed of numerically exact stable LS solutions of the isolated CQ CGL equation (corresponding to $\kappa = 0$), $U_0(\tau)$ (they were found by means of the same technique as outlined above, i.e., as attractors of the respective isolated equation). The following inputs were used at $z = 0$.

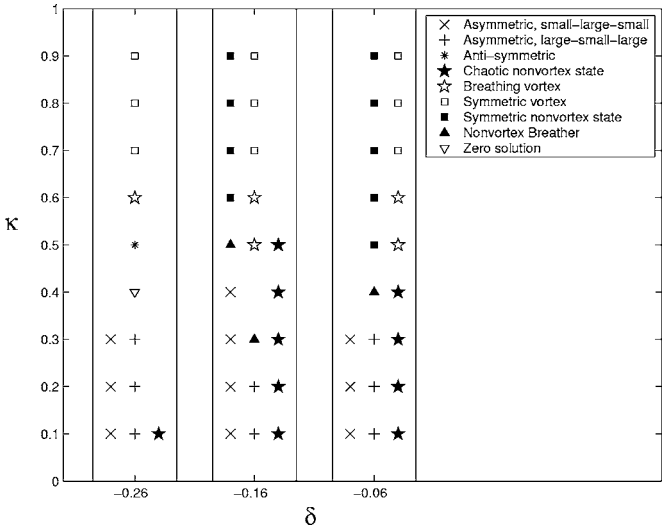

FIG. 1. The diagram of all stable localized states, in the (δ, κ) parameter plane, generated by simulations of Eqs. (1)–(3) which started with five different types of initial conditions, (i)–(v), see text. The "zero state" (symbol $\triangledown$), which appears at a single spot $(\delta = -0.26, \kappa = 0.4)$, implies that no stable nonzero solutions could be found in this case. Parameters are $\mu = \nu = 0.1$ and $\epsilon = \beta = 0.5$.

(i) A *vortex*, with $U(\tau) = U_0(\tau)$, $V(\tau) = U_0(\tau)e^{2\pi i/3}$, $W(\tau) = U_0(\tau)e^{4\pi i/3}$ (the phase shifts between the three components lend this configuration an obvious vortical structure).

(ii) *Perturbed vortices*, with $U(\tau) = 0.8U_0(\tau)$, $V(\tau) = 0.8U_0(\tau)e^{2\pi i/3}$, $W(\tau) = 1.2U_0(\tau)e^{4\pi i/3}$, or $U(\tau) = 0.8U_0(\tau)$, $V(\tau) = 1.2U_0(\tau)e^{2\pi i/3}$, $W(\tau) = 1.2U_0(\tau)e^{4\pi i/3}$, the respective coefficients 0.8 and 1.2 accounting (here and below) for the perturbation imposed on the vortex.

(iii) *Asymmetric complexes* of two types, $(0, U_0, 0)$, i.e., with $U(\tau) = W(\tau) = 0$, $V(\tau) = U_0(\tau)$, and $(U_0, 0, U_0)$, i.e., with $U(\tau) = W(\tau) = U_0(\tau)$, $V(\tau) = 0$.

(iv) *Symmetric complexes* without vorticity, with $U(\tau) = V(\tau) = W(\tau) = U_0(\tau)$.

(v) *Perturbed symmetric complexes*, with $U(\tau) = W(\tau) = 0.8U_0(\tau)$, $V(\tau) = 1.2U_0(\tau)$, or $U(\tau) = W(\tau) = 1.2U_0(\tau)$, $V(\tau) = 0.8U_0(\tau)$.

Inputs (i) and (ii) on the one side, and (iv) and (v) on the other always generated identical eventual states (which attests to the breadth of the attraction basin of those states). Thus, up to three *distinct* LS complexes may be finally observed, originating, respectively, from inputs (i) or (ii), (iii), and (iv) or (v).

All these species are included in the chart displayed in Fig. 1 (their examples are presented below). The chart features vast areas of *bistability*, and also considerable regions of *tristability*. For comparison, it is relevant to mention that a similar diagram of LSs in the system of two linearly coupled CQ CGL equations has a relatively small bistability region, and tristability (the coexistence of symmetric, asymmetric and split pulses) was, as a matter of fact, found at a single spot (corresponding to the limit case of $\delta = 0$) [16].

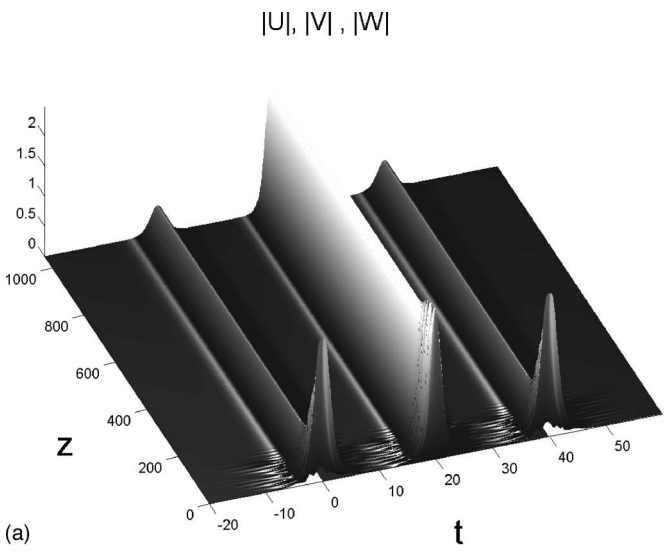

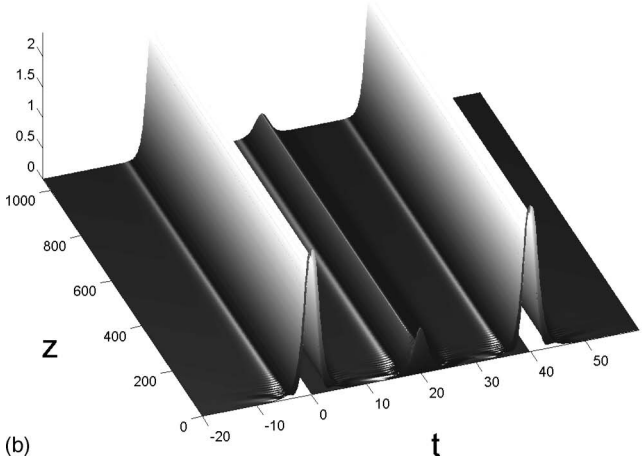

FIG. 2. Formation of stable asymmetric complexes of the "small-large-small" (a) and "large-small-large" (b) types, which correspond, respectively, to symbols "×" and "+" in Fig. 1. In either case, the initial pattern is $(U_0,0,U_0)$, belonging to type (iii), see text. Parameters are $\delta=-0.16$, $\kappa=0.4$ (a), and $\delta=-0.16$, $\kappa=0.2$ (b).

III. NONVORTICAL SOLITARY-PULSE COMPLEXES

First, we specify those types of stable states that do not carry vorticity. In Fig. 2, typical examples of the self-trapping of two different varieties of asymmetric LS complexes (with different amplitudes of the three components, "small-large-small" and "large-small-large") are displayed. They resemble stable asymmetric soliton sets found in the triangular system of FBGs [21]. In most cases, the two varieties of the asymmetric states coexist with each other, and they are found at small values of the coupling constant, $\kappa \leqslant 0.4$, which is quite natural, as the increase of κ tends to eliminate asymmetric states in systems of linearly coupled equations [16]. Note that both types of the asymmetric states in the examples displayed in Fig. 2 are generated from inputs of a single type, $(U_0,0,U_0)$, which may be naturally

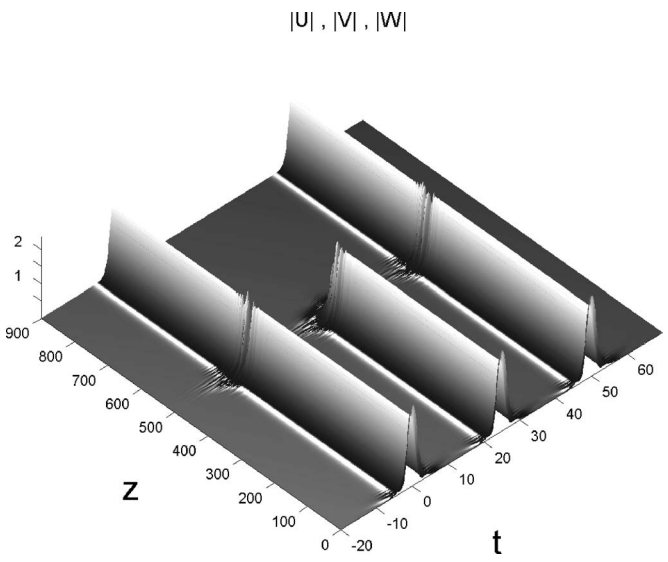

FIG. 3. Formation of a stable antisymmetric state (corresponding to symbol ∗ in Fig. 1), with one component vanishing and two others being in antiphase, through sudden onset of instability of an initial vortex configuration [of type (i), see text]. In this case, $\delta=-0.26$, ,$\kappa=0.5$. While the V component drops down and vanishes, the relative phase of the nonvanishing ones quickly changes from $2\pi/3$ to π.

classified as "large-small-large," see above. Thus, the evolution may either maintain the structure of the initial pattern or alter it [in particular, a reversal of the initial pattern is observed in Fig. 2(a), from "large-small-large" to "small-large-small"].

In addition to the two varieties of the asymmetric states, which appear at many spots in the chart of Fig. 1, a stable *antisymmetric* state, with $U=-W$ and $V\equiv 0$, was found at one spot. Straightforward inspection shows that such solutions to Eqs. (1)–(3) are indeed possible. Unlike the asymmetric states, the antisymmetric one develops as a result of an instability of the initial vortical configuration [of type (i)], see Fig. 3. Similar stable antisymmetric solutions were found in the triangular system of linearly coupled FBGs [21].

In more typical cases, instability of the initial vortex configuration (if it is unstable) leads to the emergence of (apparently) chaotic breatherlike states, as shown in Fig. 4. It cannot be excluded that, at very large z, they will slowly decay, or transform themselves into stable asymmetric complexes (the latter possibility is suggested by the fact that the chaotic breathers are observed in the range of weak linear coupling, $\kappa \leqslant 0.5$, where strongly asymmetric states dominate [16]). We stress that, although the chaotic breathers are generated from unstable vortices, they lose the vorticity, showing no persistent phase differences between the components.

In a few cases, when the asymmetric complex of the "large-small-large" type does not emerge (in fact, it exists but is unstable), in the range of $0.3 \leqslant \kappa \leqslant 0.5$, the simulations starting with the input of type $(U_0,0,U_0)$ lead to the establishment of regular breathers, which are dynamical counterparts of the asymmetric states: as shown in Fig. 5, the breather is an asymmetric complex whose shape periodically oscillates between two forms considered above, "small-large-small" and "large-small-large."

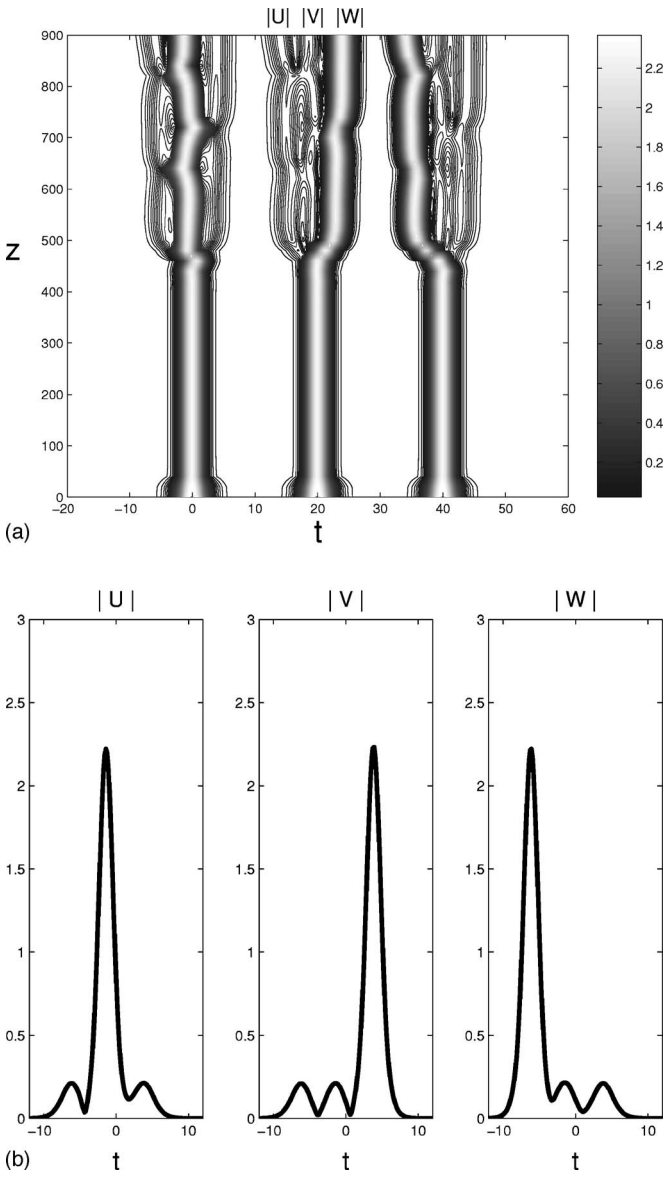

FIG. 4. (a) Formation of a chaotic breather from an unstable vortex [initial configuration (i), see text], shown by means of contour plots (which provides for a clearer picture in this case than three-dimensional images). (b) Profiles of the pattern at the end of the simulation, $z=900$. This case corresponds to symbol ★ in Fig. 1, and the example is displayed for $\delta=-0.16$, $\kappa=0.2$.

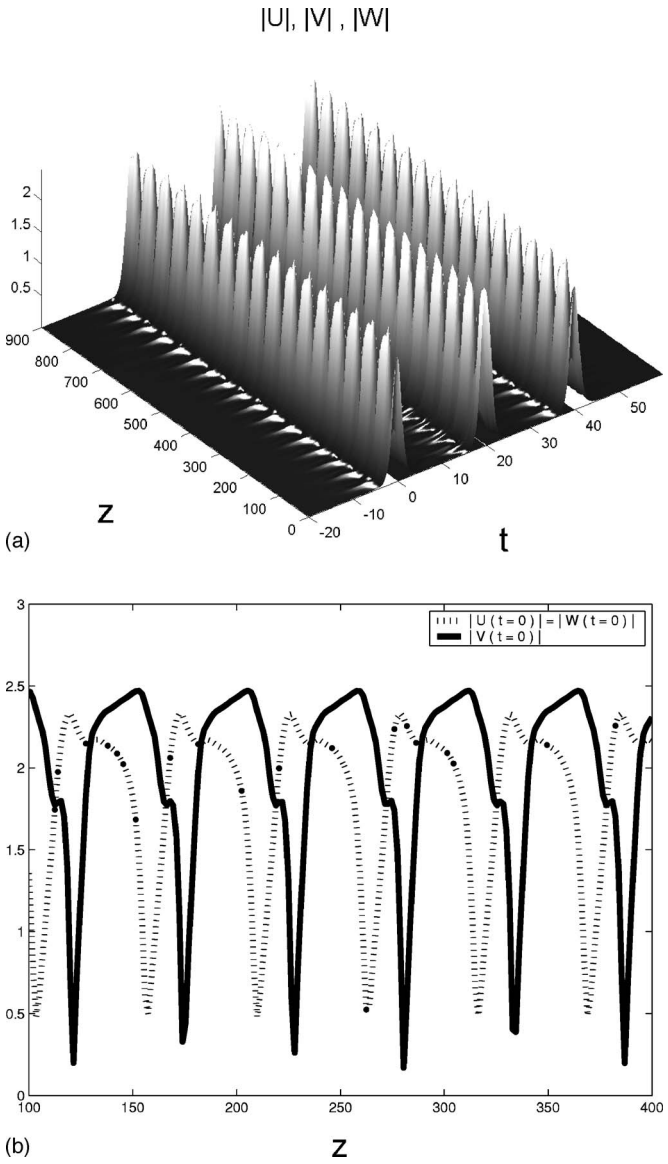

FIG. 5. (a) An example of a breather (corresponding to symbol ▲ in Fig. 1) with the V-component slightly taller than its U and W counterparts. (b) The z dependence of the amplitudes of the components V and U,W. The breather has developed from initial configuration $(U_0,0,U_0)$, of type (iii), and its shape oscillates between forms resembing two static asymmetric states shown in Fig. 2. In this case, $\delta=-0.16$, $\kappa=0.3$.

The remaining species of stable nonvortex states are symmetric complexes, with equal amplitudes of the three components (they correspond to symbol ■ in Fig. 1). We do not display examples of these states, as their shape is obvious by itself [essentially the same as in Figs. 3 and 4(a) at $z<400$].

IV. VORTICES

Vortical configurations, with (nearly) equal amplitudes of the three components, are akin to the symmetric states, in the sense that their stability may be expected at relatively large values of coupling constant κ, when the instability cannot break the symmetry between the three components. Indeed, Fig. 1 shows that both the nonvortical symmetric states and vortices may be stable at $\kappa \geqslant 0.5$, and in most cases these two species coexist, although the vortices are found to be a *single* stable species at larger values of $|\delta|$ (e.g., at $\delta=-0.26$).

In the simulations, the vortex states were distinguished from their symmetric zero-vorticity counterparts by monitoring phase differences between the components, which are $2\pi/3$ in the former case, and zero in the latter. We do not display a separate example of a completely stationary stable vortex (corresponding to symbol □ in Fig. 1), as it may be actually seen in Figs. 3 and 4(a) at $z<400$. However, it is noteworthy that, in addition to the stationary vortices, we have also found *breathing* ones, which perform stable

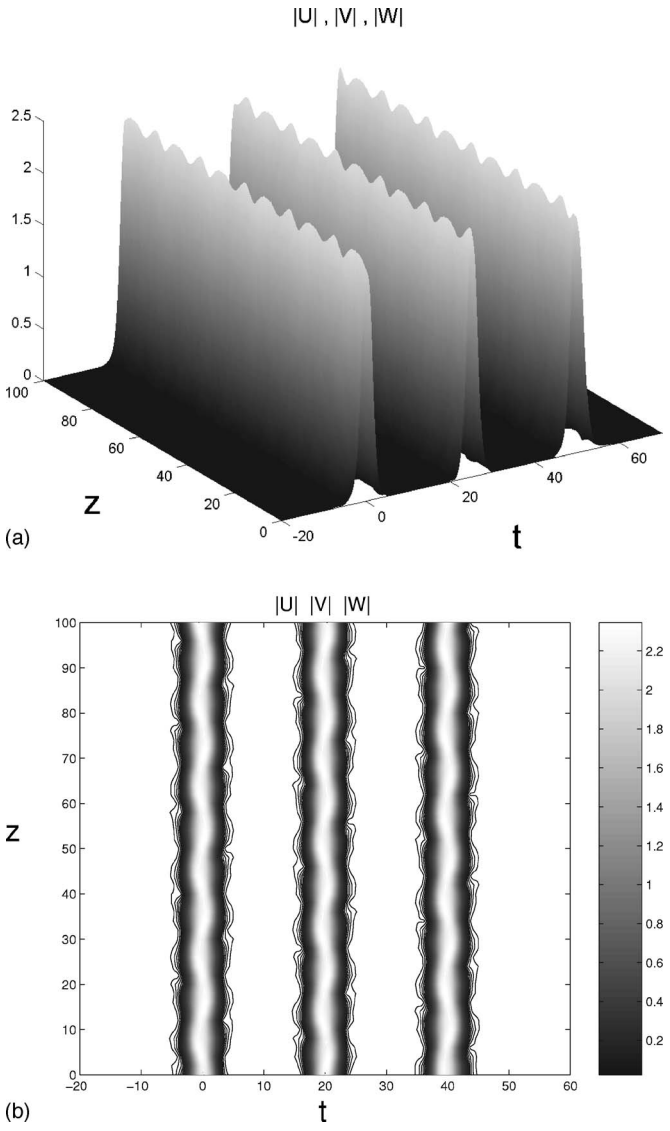

FIG. 6. (a) A typical example of a stable breathing (oscillatory) vortex, which has developed from the initial vortex configuration of type (i). (b) The same shown by means of contour plots. Analysis of numerical data confirms that this state maintains phase shifts between its three components corresponding to the vortex. Parameters are $\delta=-0.06$, $\kappa=0.5$.

periodic oscillations, as shown in Fig. 6, maintaining their vortical structure (which was checked by inspecting the phase shifts between the three components). Naturally, the breathing vortices are found at values of κ smaller than those supporting stationary vortices, as states with equal amplitudes of the three components become more fragile and amenable to perturbations at smaller κ, although they do not necessarily suffer destruction and loss of the vorticity (if any).

It is relevant to notice that rotating states (for instance, of the "small-large-small" type, with the large component switching along the cycle $U\to V\to W$), have not been found in the present model. On the other hand, rotating states were found in a model based on the two-dimensional continuous CQ CGL equation [18].

V. CONCLUSION

We have introduced a system of three cubic-quintic complex Ginzburg-Landau equations with symmetric linear couplings between them, which may serve as a simplest model of a multicore fiber laser. Stable localized states (LSs) supported by the system were identified. They subdivide in two groups: patterns of the asymmetric type, with strong difference in the amplitudes of the three components, and symmetric ones, with (nearly) equal amplitudes. Patterns belonging to these two groups are found, respectively, at smaller and larger values of the coupling constant. The full chart of the LS states features bistability and tristability.

Among symmetric LS patterns, we have found a stable vortical species, viz., triangular vortices (which may be completely stationary or periodically oscillating). In most cases, they coexist with zero-vorticity symmetric states, but a parameter region was also found where the vortices are the single stable species.

The work can be extended in various directions. In particular, since only two distinct types of vortices are possible in the triangular setting, *viz.*, ones with vorticities $S=1$ and 2, and the case of $S=1$ was explored in the present work, it remains to consider the variety with $S=2$. It may also be interesting to consider interactions between LSs (in particular, a challenging issue is the interaction between a vortex and an antivortex).

[1] I. S. Aranson and L. Kramer, Rev. Mod. Phys. **74**, 99 (2002); *Dissipative Solitons*, edited by N. Akhmediev and A. Ankiewicz (Springer, Berlin, Heidelberg, 2005).
[2] B. A. Malomed, in *Encyclopedia of Nonlinear Science*, edited by A. Scott (Routledge, New York, 2005), p. 157.
[3] F. T. Arecchi, S. Boccaletti, and P. Ramazza, Phys. Rep. **318**, 1 (1999); M. Ipsen, L. Kramer, and P. G. Sorensen, Phys. Rep. **337**, 193 (2000); P. Mandel and M. Tlidi, J. Opt. B: Quantum Semiclassical Opt. **6**, R60 (2004).
[4] F. O. Ilday and F. W. Wise, J. Opt. Soc. Am. B **19**, 470 (2000); Y. D. Gong, P. Shum, D. Y. Tang, C. Lu, X. Guo, V. Paulose, W. S. Man, and H. Y. Tam, Opt. Laser Technol. **36**, 299 (2004).
[5] L. M. Hocking and K. Stewartson, Proc. R. Soc. London, Ser. A **326**, 289 (1972); N. R. Pereira and L. Stenflo, Phys. Fluids **20**, 1733 (1977).
[6] A. J. Scroggie, W. J. Firth, G. S. McDonald, M. Tlidi, R. Lefever, and L. A. Lugiato, Chaos, Solitons Fractals **4**, 1323 (1994).
[7] V. I. Petviashvili and A. M. Sergeev, Dokl. Akad. Nauk SSSR **276**, 1380 (1984) [Sov. Phys. Dokl. **29**, 493 (1984)].
[8] B. A. Malomed, Physica D **29**, 155 (1987).

[9] O. Thual and S. Fauve, J. Phys. (Paris) **49**, 1829 (1988); S. Fauve and O. Thual, Phys. Rev. Lett. **64**, 282 (1990); W. van Saarloos and P. C. Hohenberg, *ibid.* **64**, 749 (1990); B. A. Malomed and A. A. Nepomnyashchy, Phys. Rev. A **42**, 6009 (1990); V. Hakim, P. Jakobsen, and Y. Pomeau, Europhys. Lett. **11**, 19 (1990); P. Marcq, H. Chaté, and R. Conte, Physica D **73**, 305 (1994); J. M. Soto-Crespo, N. N. Akhmediev, and V. V. Afanasjev, J. Opt. Soc. Am. B **13**, 1439 (1996); O. Descalzi, M. Argentina, and E. Tirapegui, Phys. Rev. E **67**, 015601(R) (2003).

[10] H. Sakaguchi, Physica D **210**, 138 (2005).

[11] B. A. Malomed and H. G. Winful, Phys. Rev. E **53**, 5365 (1996); J. Atai and B. A. Malomed, *ibid.* **54**, 4371 (1996).

[12] J. Atai and B. A. Malomed, Phys. Lett. A **246**, 412 (1998).

[13] H. Sakaguchi and B. A. Malomed, Physica D **147**, 273 (2000); **154**, 229 (2001).

[14] D. T. Walton and H. G. Winful, Opt. Lett. **18**, 720 (1993); E. Marti-Panameno, L. C. Gomez-Pavon, A. Luis-Ramos, M. M. Mendez-Otero, and M. D. I. Castillo, Opt. Commun. **194**, 409 (2001).

[15] H. Sakaguchi, Prog. Theor. Phys. **93**, 491 (1995); **95**, 823 (1996).

[16] A. Sigler and B. A. Malomed, Physica D **212**, 305 (2005).

[17] L. Li, A. Schülzgen, S. Chen, V. L. Temyanko, J. V. Moloney, and N. Peyghambarian, Opt. Lett. **31**, 2577 (2006); L. Michaille, C. R. Bennett, D. M. Taylor, T. J. Shepherd, J. Broeng, H. R. Simonsen, and A. Petersson, *ibid.* **30**, 1668 (2005).

[18] D. V. Skryabin and A. G. Vladimirov, Phys. Rev. Lett. **89**, 044101 (2002).

[19] F. Smektala, C. Quemard, V. Couderc, and A. Barthélémy, J. Non-Cryst. Solids **274**, 232 (2000); C. Zhan, D. Zhang, D. Zhu, D. Wang, Y. Li, D. Li, Z. Lu, L. Zhao, and Y. Nie, J. Opt. Soc. Am. B **19**, 369 (2002); K. Ogusu, J. Yamasaki, S. Maeda, M. Kitao, and M. Minakata, Opt. Lett. **29**, 265 (2004).

[20] A. V. Buryak and A. A. Akhmediev, J. Opt. Soc. Am. B **11**, 804 (1994).

[21] A. Gubeskys and B. A. Malomed, Eur. Phys. J. D **28**, 283 (2004).